Originally published as:

Wiese, B., Nimtz, M., Klatt, M., Kühn, M. (2010): Sensitivities of injection rates for single well CO2 injection into saline aquifers. - Chemie der Erde - Geochemistry, 70, Suppl. 3, 165-172

DOI: 10.1016/j.chemer.2010.05.009

Sensitivities of injection rates for single well CO_2 injection into saline aquifers

Bernd Wiese, Michael Nimtz, Matthias Klatt, Michael Kühn

Content

1 Title

Sensitivities of injection rates for single well CO_2 injection into saline aquifers

2 Authors

Bernd Wiese[a*], Michael Nimtz[b], Matthias Klatt[b], Michael Kühn[a]

[a] Helmholtz Centre Potsdam, GFZ German Research Centre for Geosciences, Centre for CO_2 Storage

[b] Chair of Power Plant Technology, BTU Cottbus, Walther-Pauer-Straße 5, 03046 Cottbus

* Corresponding author. Tel.: + 49 (0)331 288-1823, Fax: + 49 (0)331 288-1529. E-mail address: wiese@gfz-potsdam.de

3 Abstract

This paper investigates methods to predict potential injection rates of CO_2 into a saline aquifer and analyses the sensitivities of the input parameters. Geological parameters are based on conditions at the European CO_2 Onshore Research Storage and Verification Project in Ketzin, Germany and varied within an acceptable range. Two injection regimes for CO_2 are analysed: pressure controlled injection and power plant controlled injection, where the CO_2 flux depends on the load curve of a 600 MW_{net} lignite power plant. The results are determined with a numerical model and compared to an analytical solution with constant pressure injection. The injection rates depend mainly on the geological setting and only slightly on technical parameters. Aquifer permeability and thickness show approximately linear sensitivity and have a dominant impact. Depth is also of high importance, but the impact is more complex and is based on geothermal temperature and hydrostatic gradient, which affect viscosity, compressibility and caprock stability. Vertical anisotropy is insensitive. The difference in the mean rate between constant pressure injection and power plant controlled injection is 8 %. Peak injection rates are 29 % above mean injection rates, which shows that the reservoir can effectively dampen rate variations. The analytical solution predicts the highest injection rates, the lowest temporal variability and decreasing rates with injection duration. The numerical solution predicts a stronger temporal variability and the rates increase with duration. In the initial phase the differences between the methods add up to a factor of 1.45.

Keywords: CCS, injection, sensitivity, Ketzin, saline aquifer, analytical, numerical, well, rate

4 Introduction

Carbon capture and storage (CCS) is a potential method for the reduction of CO_2 emissions into the atmosphere and is believed to help mitigate global warming (IPCC 2005). The complete CCS chain consists of the separation of CO_2 from industrial and energy-related sources, transport to a storage location and long-term isolation from the atmosphere by sequestration in geological formations. Implementation of the CCS technology on the scale needed to achieve a significant impact on the reduction of CO_2 emissions requires knowledge of available CO_2 storage capacity, which is addressed in several studies (e.g. Bachu and Adams 2003, Kopp et al. 2009, Holloway 2009, Bachu et al. 2007). However, only a few studies quantify the impact of geological and technical parameters on the potential injection rates (e.g. Nordbotten et al. 2005, Mathias et al. 2009a) and these are based on analytical solutions. Nevertheless, these rates are essential for the design and operation of injection schemes. Their sensitivities depend on input parameters, which can be calculated by analytical solutions and numerical simulations. We compare both, and while analytical solutions provide fast and robust results, compared to numerical simulations they are more limited in capturing physical processes. In the present case the limitations include the assumptions of a sharp phase interface, incompressible CO_2 and a temporally invariant CO_2 injection flux. However, in the present application both methods do not consider other potentially relevant processes, such as interactions between multiple injection wells, non-isothermal effects or the limited extent of the reservoir.

To our knowledge, currently no study has estimated the potential injection rates into a deep saline aquifer taking into account the temporal variability of a CO_2 stream produced from the operation of a power plant.

In this study we perform numerical simulations to define sensitivities of potential injection rates taking into consideration a realistic power plant CO_2 load curve. The model simulates isothermal injection of CO_2 into a saline aquifer with an infinite extent. The well boundary is considered at the aquifer elevation, while the processes in the well itself are described by Nimtz et al. (2010). The storage formation is a saline aquifer whose geological parameters are constructed to match those occurring at the injection site Ketzin, Germany (Schilling et al. 2009). The simulation, which is carried out with these parameters, serves as a central point for the sensitivity analysis. The sensitivities are calculated by sequential variation of the parameters injection pressure, aquifer permeability and thickness, well diameter, vertical anisotropy and compressibility. From this sensitivity functions are derived, which can be applied to calculate the change in the potential injection rate depending on the corresponding parameter values. Furthermore simulations are carried out to assess the impact of

CO_2 compressibility and hysteresis of relative permeability. Using this procedure the most sensitive input parameters are identified and differences between analytical and numerical solutions are demonstrated.

5 Material and Methods

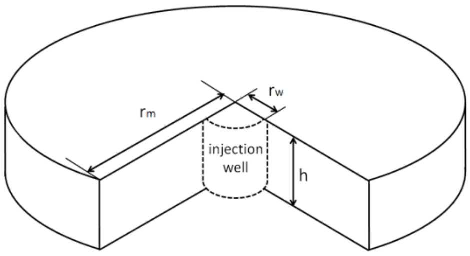

Figure 1: Model domain of the numerical models. The model is 2-D radially symmetric, r_w is the radius of the injection well, r_m the radius of the model domain, h denotes the thickness of the aquifer. Except for the injection well all boundaries are no flow.

5.1 Numerical Model

The simulations are based on a 2D radially symmetric aquifer (Figure 1). In the radial direction the domain is discretised with 100 cells. The first cell has a lateral extent of 1 m, with the extent of the next cell increasing by a factor of 1.043, resulting in a radius of 100 km. In the vertical direction the model is discretised by 25 cells using uniform spacing. The aquifer has no dip. The fully penetrating injection well is located at the centre of the domain. The properties of CO_2 are adapted from Altunin (1975), brine properties from Battistelli et al. (1997) and the partitioning of CO_2 and brine is calculated according to Spycher and Pruess (2005). Outer boundary conditions are no flow, while it is ensured that the aquifer emulates infinite extent (see below). Simulations are isothermal and carried out with the simulator E100 Version 2008.2 (Schlumberger 2009).

5.2 Analytical Solution

Mathias et al. (2009a) provide an analytical solution for the injection pressure p . The solution represents the injection of CO_2 into an infinite brine aquifer with a sharp interface between both phases. The aquifer is homogeneous and only a single permeability can be applied for both CO_2 and brine. For each phase a viscosity can be specified, but the application of compressibility is limited to brine and rock while CO_2 is assumed to be incompressible. The solution includes Forchheimer flow for the CO_2 phase. It is not possible to simulate a power plant controlled injection regime. The solution is developed for constant rate injection but nevertheless, a slightly variable rate for constant injection pressure is determined by iteration with sufficient accuracy. The pressure slightly increases during the injection period and consequently the maximum pressure is reached at the end of the period. For a shorter duration a higher mass flow is possible. A quasi transient mass flow is calculated as a sequence of maximum injection rates with a shorter duration. The difference in the cumulative mass flows between both approaches is less than 1 %. This difference in the cumulative injection mass is corrected by scaling the time to the cumulative mass injection.

5.3 Simulation parameters

The parameter set is constructed to mimic the conditions at the Ketzin test site, provided in Table 2. The formation properties permeability and compressibility of 7.2×10^{-5} bar^{-1} are taken from Wiese et al. (2010). Formation thickness and porosity are derived from Norden et al. (2010). The vertical anisotropy is estimated based on permeability values from Norden et al. (2010).

The relative permeability formulation follows the Corey approach (1954)

$$k_{ri}(S_i) = K\left(\frac{(S_i - S_{i,residual})}{(1 - S_{i,residual} - S_{j,residual})}\right)^{n_i}$$ **Equation 1**

With k_{ri} as the relative permeability of phase i, K as (saturated) permeability, S_i the actual saturation of phase i, $S_{i/j,residual}$ the residual saturation of the respective phase and n_i a dimensionless exponent. The phase i may represent either CO_2 or brine and therefore j represents the other phase. For parameterisation the values listed in Table 1 were used. These are mean values from the parameter range proposed by Schepernisse and Maas (2009) based on measurements of sandstone cores at the Ketzin test site.

The resulting relative gas permeabilities for residual gas saturation differ for drainage and imbibition. For consistency both values are set to 0.6. The other parts of the curves are scaled proportionally. The resulting relative permeabilities (Figure 2) are applied to the model. The capillary pressure is simulated in the same way for drainage and imbibition and follows Equation 2 with S_w as the wetting phase saturation and the parameter values a= 0.096, b= 0.125 and n= -0.989.

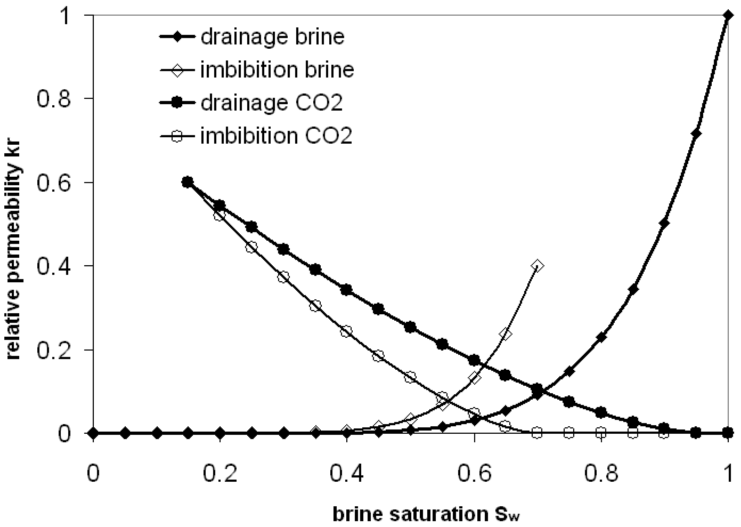

Figure 2: Relative permeabilities of brine and CO_2. Residual brine saturation is 15%.

$$p_c = \left(\frac{S_w - b}{a} \right)^n \quad \textbf{Equation 2}$$

The PVT properties of CO_2 change with depth. For the applied geothermal and hydraulic gradient (Table 2) between 642 m and 1000 m density and viscosity increase up to 134 % and 114 %, respectively, while the increase between 1000 m and 2000 m is only 5 % and 10 %, respectively. The depth of 1000m is chosen as the central point because here the PVT properties are separated in a high variation region for shallower conditions and a low variation region for deeper conditions. Since saline aquifers frequently have a lower salinity than at Ketzin the salinity was slightly decreased to the round number of 20 %. The permitted injection overpressure at Ketzin is 22.9 bar (Köhler, 2009), so a feasible (round number) pressure of 20 bar is adopted at the central point.

The CO_2 load curve is adapted from a basic load 600 MW_{net} lignite power plant with 4 blocks. The base length is 365 days, which is repeated for a time series of 20 years. The maximum and minimum rates are 29 % above and 50 % below the mean annual rate, respectively.

For comparison with the analytical solution numerical simulations with incompressible CO_2 are carried out. For these cases and for the analytical solutions PVT properties for both phases are adapted to meet the equilibrium conditions of the aquifer.

5.4 Characteristic injection rates

For all solutions the injection rate $\dot{m}(t)$ is time variant. Characteristic injection rates are calculated with Equation 3 to ensure comparability. Depending on the limits t_1 and t_2 different characteristic rates are obtained.

$$\bar{\dot{m}}_i = \frac{1}{t_2 - t_1} \int_{t_1}^{t_2} \dot{m}_i(t)\, dt \qquad \textbf{Equation 3}$$

The times t_1 and t_2 define the respective interval and $\bar{\dot{m}}_i$ is the characteristic injection rate. The mean injection rate for the numerical solution is denoted $\bar{\dot{m}}_{num,cp}$ for constant pressure injection, $\bar{\dot{m}}_{num,pp}$ for power plant controlled injection and $\bar{\dot{m}}_{a,cp}$ for the analytical solution (which implies constant pressure). All mean injection rates are obtained with t_1=0 and t_2=20 years. When the injection is pressure controlled $\dot{m}(t)$ is always the maximum for the time interval and can also be used to set up temporal regression. For power plant controlled injection the determination of temporal regression requires that the actual rate $\dot{m}_{num,pp}(t)$ be scaled in order to ensure that the reservoir can sufficiently buffer the fluctuations so that they do not induce a higher pressure than allowed. The parameter $\bar{\dot{m}}_i$ in equation 3 is time dependent for power plant controlled injection, denoted as $\bar{\dot{m}}_{num,pp}(t)$ and calculated as a window function with the length of the window t_2-t_1 equal to the base length of the load curve, which is 365 days and $t = t_1$.

5.5 Sensitivity analysis

Based on one central point a picture of the impact of each parameter is obtained by variation of one parameter for each simulation (Table 3) while keeping the other parameters constant. However, if several parameters change simultaneously the sensitivity of individual parameters may change due to the nonlinear nature of the processes. Formerly insensitive parameters may become sensitive or vice versa. In order to account for these effects the insensitivity of domain and discretisation are double checked for the highest and lowest injection rates.

Simulations are carried out to ensure that the bottomhole pressure does not exceed the feasible pressure. A constant well pressure is set as boundary condition, for which a transient injection rate is computed by the simulator. This procedure is not applicable for power plant controlled injection. The injection rate is given by the power plant load curve and most of the time the well pressure is below the feasible pressure. The feasible pressure is only reached during short periods, because the constant pressure boundary cannot be used since it would affect the injection rate. The task is to scale the characteristic rate $\overline{\dot{m}}_{num,pp}(t)$ so that the feasible pressure is reached exactly at the injection peaks. This cannot be carried out by the simulator. The scaling factor is determined by two regression functions instead, which are calculated using values from the annual maximum pressure. Four simulations with different mean injection rates are carried out with annual maximum pressures on both sides of the feasible pressure (an iterative approach). From the temporal regression (see below) it is known that the break-even point (when $\overline{\dot{m}}_{num,pp}(t)$ is equal to $\overline{\dot{m}}_{num,pp}$) will be reached after 7 years. Based on this the feasible mean injection rate $\overline{\dot{m}}_{num,pp}$ is determined.

One simulation is carried out with the mean injection rate $\overline{\dot{m}}_{num,pp}$ for the entire duration. The maximum pressure p is determined for each year. The inverse of the regression function through p describes the temporal scaling for the injection rate. The first year is not included because the base length of the power plant load curve is one year and because the pressure fluctuations are too high to be accurately described with the present approach.

Different formulations are applied when fitting the sensitivities, with preference given to the simplest formulation that provides the minimal deviation. Most formulations could be fitted with linear and exponential functions.

Polynomial formulations would provide a perfect fit for up to 3 points, but they would potentially include a local maximum. Therefore exponential regression functions were applied and set up with respect to physical behaviour. They include the zero-zero point when reasonable, for example no CO_2 is injected at zero injection pressure. The temporal sensitivity of power plant controlled injection requires a more sophisticated regression formulation including three parameters, a reciprocal and a logarithm. The regressions are fitted by a minimisation of the sum of the squared residuals, using the software R (www.r-project.org).

6 Results

6.1 Model convergence

The results from the model are insensitive with regard to discretisation. Further refinement by a factor of 10 (1 m to 0.1 m) does not change the injection rate, while an increase by a factor of 5 reduces the injection rate by 2 % (191 t/d to 187 t/d). The extent of the model is proven to be large enough to mimic an infinite extent aquifer. When increasing the radius from 100 km to 1000 km with the identical number of cells and the identical size of the cells next to the well, the injection rate for the central point is not affected. Also, for the simulation with the highest injection rate, the latter increase in radius affects the potential injection rate by only 0.4 %, which is considered not to be significant.

6.2 General behaviour

Pressure controlled numerical solution

In the numerical solution with pressure controlled injection at the very beginning (t<2min) of injection the actual injection rate is about twice as high as the mean rate. Later (t<=1d) the rate decreases to about 70 % of the mean injection rate and then stabilises after 1 day of injection. Beginning from day 30 until the end of the simulation at 20 years the injection rate increases by 10 %, with the maximum at the end of injection (Figure 3).

The regression curve for temporal behaviour is shown in Figure 3. Beginning from day 10 the injection rates are reproduced with sufficient accuracy. They follow an exponential function (Table 4) with a mean numerical injection rate $\overline{\dot{m}}_{num,cp}$ of 193 t/d. At 2598 days (7.1 years) the break-even point is reached, whereby the actual injection rate $\dot{m}_{num,cp}(t)$ is identical to the mean injection rate $\overline{\dot{m}}_{num,cp}$.

Pressure controlled analytical solution

The analytical solution shows some important differences. The mean injection rate $\overline{\dot{m}}_{a,cp}$ is 233 t/d, which is 21 % higher than in the numerical solution. At all times the rates are higher than calculated with the numerical model. The main reason is that the relative permeability of CO_2 is always equal to 1, whereas it has values of between 0 and 0.6 in the numerical solution and that the CO_2 phase is considered to be incompressible. In contrast to the numerical model, the injection rate decreases continuously. At 2957 days (8.1 years) the break-even point is reached and the actual injection rate $\dot{m}_a(t)$ is identical to the mean injection rate $\overline{\dot{m}}_a$.

Power plant controlled numerical solution

The maximum mean injection rate for the power plant load curve $\overline{\dot{m}}_{num,pp}$ is 178 t/d, which is 8 % lower than in the numerical solution with constant injection pressure. During the first year the injection is simulated at a constant rate because the reservoir potential to dampen load curve oscillations is reduced if the mass of reservoir CO_2 is too small. Injection fluctuations should be especially avoided during this time. Similar to the numerical solution with constant pressure, the injection potential continuously increases with time. At 2949 days (8.1 years) the actual injection rate $\overline{\dot{m}}_{num,pp}(t)$ is identical to the mean injection rate $\overline{\dot{m}}_{num,pp}$.

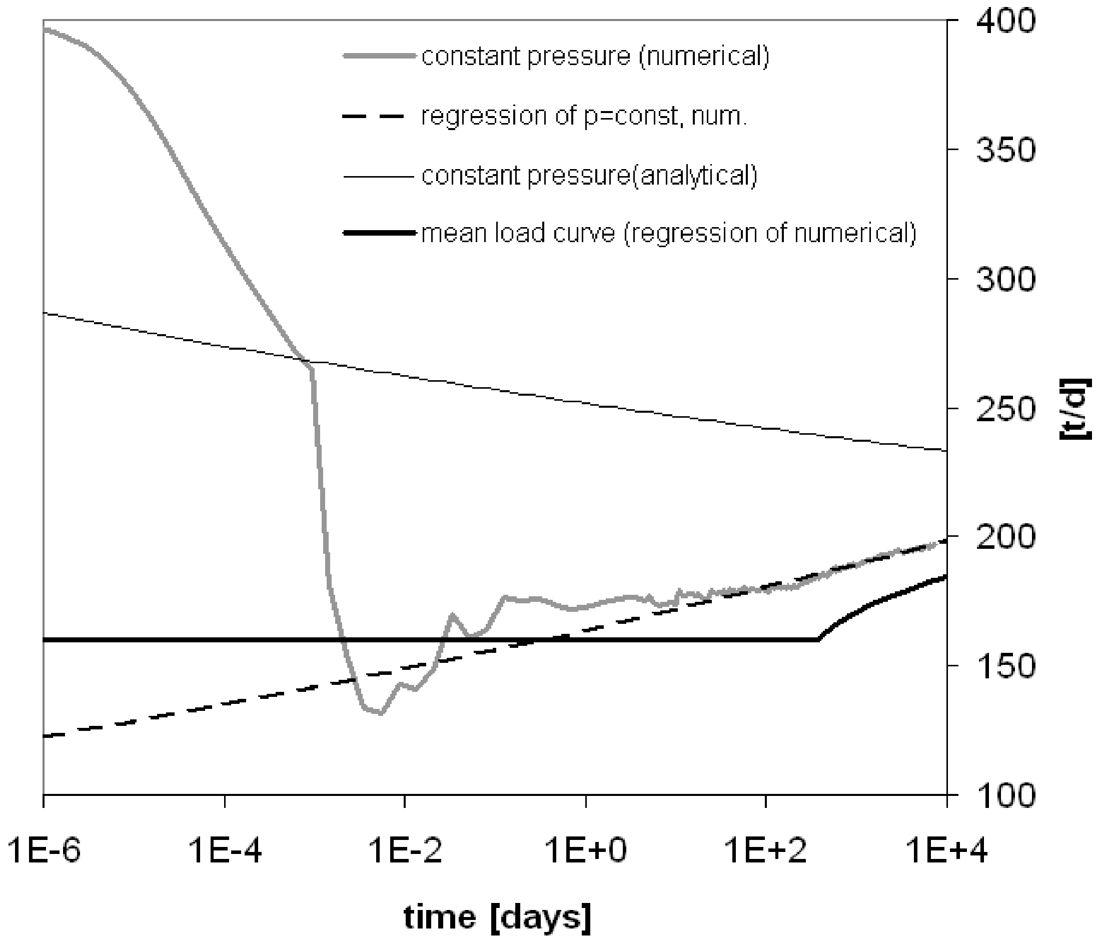

Figure 3: Temporal injection rate at the central point, calculated with the numerical model and the analytical solution. The regression function corresponds to the numerical model.

6.3 Sensitivities

All sensitivities (eight) have been calculated with the numerical solution of constant pressure injection. With the analytical solution only six sensitivities could be calculated, as due to the limitations it was not possible for vertical anisotropy and for power plant controlled injection to be calculated. For power plant controlled injection only two sensitivities are determined, those for the pressure and duration of injection.

The impact of the parameters on the injection rate is presented in Table 4. Except for anisotropy and temporal dependence an initial estimation could be carried out applying linear sensitivities. On the other hand, except for permeability and aquifer thickness, a nonlinear fit provides increased accuracy. The exponent of the nonlinear sensitivity shows the grade of nonlinearity.

For the purpose of design sensitivities have to be considered in conjunction with respective parameter variability. From this point of view the most important parameter is aquifer permeability. The injection rates are almost proportional to this parameter and the high variability results in an absolute sensitivity of 0.1 to 10.2 (Table 4). Sensitivity differences between the analytical solution and numerical solution are small.

Injection pressure has the second highest impact on the mean injection rates. They are nearly proportional to the pressure for both constant well pressure and power plant injection, but for the analytical solution the exponent of 1.158 exhibits a considerable non-linear rate dependence. Doubling injection pressure increases the injection rate by a factor of 2.23. This is because intermediate saturations do not exist and therefore relative permeabilities are always equal to one. With compressible CO_2 the nonlinearity would be even stronger. The mean injection rate is proportional to aquifer thickness. The sensitivities are identical for numerical and analytical solutions, which show that buoyancy effects are negligible.

The potential injection rate increases by a factor of about 1.8 for reservoir depths between 650 m and 2000 m in the numerical solution. The viscosity of the brine decreases with higher temperature at a greater depth, but the density of the brine hardly changes. For the CO_2 phase the temperature effect is compensated by the higher pressure, i.e. density and viscosity increase roughly simultaneously, so that flow resistance per mass flux remains roughly constant (± 5 %). However, for the same mass, the specific injection volume becomes more important for shallow depths because the density of CO_2 increases by 134 % between 650 m and 1000 m and only by 5 % between 1000 m and 2000 m. Therefore the volume flux is much higher and more brine has to be replaced for the same mass of CO_2. Furthermore, the rate decrease for shallow injection is much more pronounced in the analytical solution because the CO_2 phase is treated as incompressible. By contrast, in the numerical solution the compressibility of the CO_2 increases significantly with depth and hence leads to a higher storage coefficient for shallow aquifers. This decreases the radius of influence and therefore allows a higher injection rate. Numerical simulations show that the assumption of incompressible CO_2 reduces injection rates by 5% at 1000 m depth and by 51% at 650 m depth.

Increasing rock compressibility allows higher injection rates with a parameter range variability factor of 1.5 to occur. The reason is again due to higher compressibility decreasing the radius of influence. The impact of rock compressibility is highest for the deepest scenario where the total compressibility (sum of CO_2, brine and rock) is smallest. Since CO_2 compressibility is disregarded rock compressibility has the highest impact on the radius of influence in the analytical solution, with a variability factor of 1.72 (Table 3).

The injection rate changes with the duration of the injection. The trend can be described with an exponential function, leading to a much higher impact at the beginning of injection than at the end. In the numerical solutions the potential rate increases, while it decreases in the analytical solution. The decrease occurs due to the reduced relative permeability at intermediate phase saturation, where CO_2 and brine obstruct each other. The sum of both relative permeabilities is significantly lower than one (Figure 3). With increasing time this region migrates further from the injection well and has a lower impact. Numerical simulations show that the assumption of incompressible CO_2 hardly affects temporal behaviour at the central point.

The rate of reduction is more pronounced for power plant controlled injection. After one year $\overline{m}_{num,pp}(t)$ is only 90 % of $\overline{m}_{num,pp}$, while $\dot{m}_{num,cp}(t)$ is 96 % of $\overline{m}_{num,cp}$. Later the dampening effect of increased storativity becomes more important. After 20 years $\overline{m}_{num,pp}(t)$ is 103 % of $\overline{m}_{num,pp}$ and $\dot{m}_{num,pp}(t)$ is 102 % of $\overline{m}_{num,pp}$.

In the analytical solution neither relative permeability nor compressibility are incorporated. Therefore it behaves more like an ordinary pumping test and the rate decreases continuously with constant pressure injection. The rate difference is smaller than in the numerical solution, equalling only 7 % between 1 day and 20 years.

For load curve controlled injection the overpressure is below the feasible pressure for most of the time. Therefore, the mean injection rate is 8 % lower compared to constant pressure injection. Nevertheless, due to periods of low injection, it is possible to increase the rate for short periods by about 19 % above the pressure controlled rate. Because maximum injection pressure also depends on the rate history it does not occur at the maximum injection rate, but the rates are within a range of 3 % below maximum.

Several parameters show a very low sensitivity. Hysteresis does not affect the injection rate. Slight pressure differences occur for power plant controlled injection during phases when the rate is low and the well pressure is far below the feasible value. Physically this is reasonable, the injection never ceases and therefore drainage is the dominant process. The pore pressure is also practically insensitive. When disregarded the injection rates decrease by only 2 %. Also the sensitivity of the well diameter is low. A change by more than a factor of 4 results in a 4 % difference in the injection rate.

7 Discussion

The present study allows quantification of the potential mass flow of CO_2 during well injection with a constrained maximum injection pressure. All methods provide mean rates which are within a variation range of 30 %. The analytical method of Mathias et al. (2009b) provides the largest predicted value $\overline{\dot{m}}_{a,cp}$ of 233 t/d. However this solution tends to overestimate the rates because it does not consider permeability reduction due to relative permeabilities, and also tends to underestimate the rates because the CO_2 is assumed to be incompressible. With the numerical model both effects are considered and a mean injection rate $\overline{\dot{m}}_{num,cp}$ of 193 t/d can be achieved, which shows that the latter effect is dominant at the applied central point for a depth of 1000 m. Additionally the fact that the CO_2 load curve displays temporal variations because it depends on the load curve of a power plant must be considered. With a realistic load curve an injection rate $\overline{\dot{m}}_{num,pp}$ of 178 t/d can be achieved. This is 30% lower than the prediction from the analytical method. Nevertheless, considering the numerous impacting factors on the potential injection rate, the relevance of this difference should not be overestimated.

The temporal behaviour differs for the three approaches. In the analytical solution the temporal development of the injection rate shows only a slight decrease. The rate has the minimum value at the end of the injection period, where it is only 199 % of the mean rate, while an increase is predicted in the numerical solutions for constant pressure and power plant load curve with 102 % and 103 % of the mean injection rates, respectively. The initial behaviour is more important. For constant pressure injection after one year 96 % of the mean injection rate $\overline{\dot{m}}_{num,cp}$ can be achieved and the ratio is only 90 % of $\overline{\dot{m}}_{num,pp}$ for the power plant controlled rate. For the latter case it must be taken into account that during the first year the injection rates are constant, otherwise the ratio would be much lower.

The predicted rates depend on the prediction tool. The analytical solution shows an unrealistically high depth sensitivity for depths shallower than 1000 m. At 650 m the rates are 68% lower, while the numerical solution provides results that are only 21 % lower than the respective rates at the central point. The difference of 47 % occurs because at shallow depths CO_2 is highly compressible. If this is neglected the radius of influence is much higher, whereby injection rates are much lower. At greater depths the difference is only 3 % because CO_2 compressibility decreases significantly. A slight overestimation of injection pressures (in our case underestimation of the rates) was expected by Mathias et al. (2009b) since the assumption of incompressible CO_2 is not strictly valid for the temperature and pressure regions which typically occur during CO_2 sequestration. It can be affirmed that the effect occurs, but it must be emphasised that the effect is much more pronounced for shallow depths. Due to incompressible CO_2 the analytical solution is also more sensitive to rock compressibility, but the difference between the methods is only between 2 % and 15 %. Nevertheless, rock compressibility shows moderate sensitivities to the rates and may have an impact factor of 1.5.

The geological situation has a much higher impact than the prediction method. The most important parameters are hydraulic permeability and aquifer thickness. The injection rate is proportional to these values, but since hydraulic permeability varies by several orders of magnitude aquifer thickness has less of an impact. Caprock stability defines the maximum feasible injection pressure and the stability itself depends on depth. As a rule of the thumb feasible pressure increases linearly with hydrostatic pressure (Birkholzer et al. 2009) or with lithostatic pressure (Hovorka et al. 2004), whereas sustainable injection pressure increases linearly with depth. The mean injection rate is nearly proportional to the pressure for both constant well pressure and power plant injection. Taking this into consideration the potential injection rate between 1000 m and 2000 m increases by a factor of about 2. Additionally higher temperatures cause lower brine viscosity, which increases the potential injection rate by a factor of about 0.5. Altogether the depth related effects add up to a factor of 2.5 for the increase in the potential injection rate between 1000 and 2000 m.

The technical means to increase injection rates are limited. The only parameter which is not directly or indirectly affected by geological properties is the borehole diameter. However, within a reasonable range, the absolute sensitivity is only 4 %. In reality this could be slightly higher because the analysed approaches do not include drying due to brine evaporation.

Technical injection schemes imply a temporal change in the CO_2 load curve. For the present load curve the peak injection rate $\dot{m}_{num,pp}(t)$ is 29 % higher than the mean, but the mean injection rate $\overline{m}_{num,pp}$ is only 8 % lower compared to the pressure controlled rate $\overline{m}_{num,pp}$ since reserves are built up during times of lower injection. The peak injection rate $\dot{m}_{num,pp}(t)$ may be 19 % higher than the mean injection rate $\overline{m}_{num,cp}$, which also means that technical solutions to decrease the peak rate have an impact potential of less than 8 % on the mean injection rate. Nevertheless, at the beginning peak loads should be decreased by technical measures to rapidly achieve a certain amount of $CO_{2,}$ which can effectively dampen the pressure response of the rate variations.

The geological setting is adapted to the unfavourable Ketzin conditions. A mean injection rate $\overline{m}_{num,pp}$ of 178 t/d might appear to be low but this value is highly sensitive to a number of parameters. In storage formations permeabilities are frequently higher (Kopp et al. 2009). Also aquifer thickness and maximum injection pressure (Mathias et al. 2009b) may have considerably higher values. For more favourable conditions, namely higher permeability, greater thickness and depth, and considering the respective sensitivities, injection rates of 1000 t/d or greater are within a realistic scope.

As an initial approximation the potential injection rate may be assumed proportional to the values for permeability, aquifer thickness and injection pressure, which allows sensitivity to be determined with just one simulation. This may not be strictly valid, and also depends on the characteristics of the actual relative permeability function. In the analytical solution for example it is not included, therefore injection rate increases more than proportionally with pressure.

This study is based on the assumption of single well injection. When injection is carried out with multiple wells their pressure cones would intersect and reduce the usable injection overpressure. The present assumption of an infinite extent aquifer is optimistic. When the extent of the aquifer is limited, namely a reservoir, it will be necessary to install relief wells to avoid a rapid increase in reservoir pressure and the decrease in usable injection overpressure. Both effects counteract the increasing potential injection rate with time.

8 Conclusions

Injection rates were predicted and the sensitivities of different geological, technical and operational parameters were determined with respect to achievable mass flow for single well CO_2 injection into a saline aquifer. The relevance of the parameters is assessed by applying a reasonable parameter range for the sensitivity function. The central point of the analysis was constructed to mimic conditions at the Ketzin test site. For these conditions a mean injection rate $\overline{\dot{m}}_{num,pp}$ of 178 t/day can be achieved for power plant controlled injection.

The impact of the prediction method should be considered. The analytical solution provides the most optimistic prediction for both injection rates and temporal behaviour, while the numerical simulation with a power plant controlled injection rate provides the most realistic behaviour, but with the smallest mean rate and the highest temporal variability of the annual mean injection rate. These effects may add up to a difference in the rate factor of 1.45.

Injection rates are nearly proportional to aquifer permeability, which is the most important influencing factor due to its high variability. Aquifer thickness also shows linear sensitivity, resulting in considerable impact. The sensitivity of aquifer depth between 1000 m and 2000 m equals a factor of 2.5. This is a combined effect resulting from different CO_2 and brine properties due to changing temperatures and hydrostatic pressures, but the depth dependent increase in the feasible injection pressure is more important.

Rock compressibility shows a moderate sensitivity and may increase injection rates for highly compressible aquifers by about one third. It is of minor importance to consider vertical anisotropy, pore pressure and hysteresis, as their impact on injection rate is each less than 5 %. The insensitivity of anisotropy shows again that the system is dominated by horizontal flux and that buoyancy effects are negligible.

During the initial phase the reservoir reacts sensitively to variations in the injection rate. During this phase the rate should be held constant in order to avoid large pressure variations and to ensure that the reservoir contains enough mass of CO_2 to effectively dampen rate variations at a later time. In the current example, for one year and later, the injection rate may be increased by just 8 % if all rate variations could be levelled out. This implies that a transient injection regime allows periods with injection rates above the mean. For the applied realistic power plant CO_2 load curve the peak rate may be 29 % higher than the mean and 19 % above the pressure controlled rate. The borehole diameter has a minor impact. Within a reasonable range of between 5 cm and 21.6 cm the well diameter has an impact of less than 4%.

The study shows that injection rates depend mainly on the geological setting and the analysed technical measures have only a slight impact. However, the interaction of multiple wells, which may considerably affect the potential injection rate, are not taken into account.

9 Nomenclature

A [-] vertical aquifer anisotropy
a [-] capillary pressure parameter
b [-] capillary pressure parameter
d [cm] well diameter
$k_{r,i}$ [-] relative permeability, for i as CO_2/Brine
n_i [-] Corey parameter, for i as CO_2/Brine
h [m] aquifer thickness
K [mD] aquifer permeability
$\dot{m}_i(t)$ [t/d] actual injection rate, with i=num,cp: numerical constant pressure injection, i=num,pp: numerical, power plant controlled, i=a,cp analytical, constant pressure injection
$\overline{\dot{m}}_i$ [t/d] mean injection rate for entire period with i=num,cp: numerical constant pressure injection, i=num,pp: numerical, power plant controlled, i=a,cp analytical, constant pressure injection
$\overline{\dot{m}}_{num,pp}(t)$ [t/d] mean mass injection rate for power plant controlled injection, determined for a one year interval beginning with time t.
n [-] capillary pressure parameter
p [bar] injection overpressure (above hydrostatic pressure)
p_c [Pa] capillary pressure
r_w [m] well radius
r_m [m] model radius
S [1/bar] rock compressibility
S_i [-] saturation, for i as CO2/Brine
$S^j_{i,residual}$ [-] residual saturation with i as the phase CO2/Brine and j as drainage/imbibition
t [d] time
ϕ [-] aquifer porosity

10 Acknowledgements

The study was carried out within the framework of the GeoEn project (www.geoen.de), financed by the BMBF (German Federal Ministry of Education and Research). The authors are grateful to Caroline Stott (BTU Cottbus) for linguistic revision of the text.

11 References

Altunin, V., 1975. Thermophysical Properties of Carbon Dioxide (in Russian). Publishing House of Standards, Moscow, 551.

Bachu, S., Adams, J., 2003. Sequestration of CO2 in geological media in response to climate change: capacity of deep saline aquifers to sequester CO2 in solution. Energy Convers. Manage. 44 (20), 3151-3175.

Bachu, S., Bonijoly, D., Bradshaw, J., Burruss, R., Holloway, S., Christensen, N.P.,Mathiassen, O.M., 2007. CO2 storage capacity estimation: Methodology and gaps. Int. J. Greenhouse Gas Control 1 (4), 430-443.

Battistelli, A., Calore, C.,Pruess, K., 1997. The simulator TOUGH2/EWASG for modelling geothermal reservoirs with brines and non-condensible gas. Geothermics 26 (4), 437 - 464.

Birkholzer, J.T., Zhou, Q.,Tsang, C.-F., 2009. Large-scale impact of CO2 storage in deep saline aquifers: A sensitivity study on pressure response in stratified systems. Int. J. Greenhouse Gas Control 3 (2), 181 - 194.

Corey, A., 1954. The Interrelation Between Gas and Oil Relative Permeabilities. Producers Monthly 19, 38-41.

Holloway, S., 2009. Storage capacity and containment issues for carbon dioxide capture and geological storage on the UK continental shelf. Proceedings of the Institution of Mechanical Engineers Part A - Journal of Power and Energy 223 (A3, Sp. Iss. SI), 239-248.

Hovorka, S.D., Doughty, C., Benson, S.M., Pruess, K.,Knox, P.R., 2004. The impact of geological heterogeneity on CO2 storage in brine formations: a case study from the Texas Gulf Coast. Geological Society, London, Special Publications 233, 147-163.

IPCC, (2005) IPCC Special Report on Carbon Dioxide Capture and Storage. Prepared by Working Group III of the Intergovernmental Panel on Climate Change [Metz, B., O. Davidson, H. C. de Coninck, M. Loos, and L. A. Meyer (eds.)]. Cambridge University Press, Cambridge, United Kingdom and New York, NY, USA, 442 pp.

Kopp, A., Class, H.,Helmig, R., 2009. Investigations on CO2 storage capacity in saline aquifers—Part 2: estimation of storage capacity coefficients. Int. J. Greenhouse Gas Control 3, 277-287.

Köhler, S., Zemke, J., 2009. 1. Zwischenbericht zum Reservoirmonitoring im Rahmen des Projektes "CO2Sink" am Standort Ketzin - Zeitraum Juni 2008 bis Dezember 2008. , UGS - Untergrundspeicher- und Geotechnologie- Systeme GmbH.

Mathias, S.A., Hardisty, P.E., Trudell, M.R.,Zimmerman, R.W., 2009. Screening and selection of sites for CO2 sequestration based on pressure buildup. Int. J. Greenhouse Gas Control 3 (5), 577-585.

Mathias, S., Hardisty, P., Trudell, M.,Zimmerman, R., 2009. Approximate Solutions for Pressure Buildup During CO2 Injection in Brine Aquifers. Transp. Porous Media 79 (2), 265-284.

Nimtz, M, Klatt, M., Wiese, B., Kühn, M. Krautz, H.-J. Modelling of the CO_2 process- and transport chain in CCS systems - Examination of transport and storage processes, submitted to Chemie der Erde, this issue

Nordbotten, J.M., Celia, M.A.,Bachu, S., 2005. Injection and Storage of CO2 in Deep Saline Aquifers: Analytical Solution for CO2 Plume Evolution During Injection. Transp. Porous Media 58 (3), 339-360.

Norden, B., Förster, A., Vu-Hoang, D., Marcelis, F., Springer, N.,Le Nir, I., 2010. Lithological and petrophysical core-log interpretation in the CO2SINK, the european CO2 onshore research storage and verification project. SPE Reservoir Evaluation & Engineering 13 (2), 179-192.

Scherpenisse, W., Maas, J., 2009. Ketzin relative permeabilities and capillary pressures. , Shell.

Schilling, F., Borm, G., Würdemann, H., Moller, F.,Kuhn, M., 2009. Status Report on the First European on-shore CO2 Storage Site at Ketzin (Germany). Greenhouse Gas Control Technologies 9 1 (1), 2029-2035.

Schlumberger (2009), Eclipse 2008.2 Technical Description, Schlumberger LTD

Spycher, N., Pruess, K., 2005. CO2-H2O mixtures in the geological sequestration of CO2. II. Partitioning in chloride brines at 12-100°C and up to 600 bar. Geochim. Cosmochim. Acta 69 (13), 3309-3320.

Wiese, B.; Böhner, J.; Enachescu, C.; Würdemann, H.; Zimmermann, G. 2010 Hydraulic characterisation of the Stuttgart Formation at the Ketzin test site, special issue of International Journal of Greenhouse Gas Control, submitted

12 Tables

Table 1: Corey parameters for CO_2 and brine for drainage and imbibition.

Corey parameters	CO_2	Brine
n	1.5	5.5
$S^{i}_{r,imb}$	0.3	0.15
$S^{i}_{r,drn}$	$S^{CO2}_{r,drn} = 0.05$ $S^{bri}_{r,drn} = 0.05$	0.15

Table 2: Aquifer parameters at the Ketzin test site and corresponding values at the central point.

	Ketzin	Central point of sensitivity study
Well diameter, r_w	21.59 cm	21.59 cm
Permeability, K	40-110 mD	100 mD
Porosity, ϕ	0.26	0.26
Relative permeability, $k_{r,co2}$, $k_{r,brine}$	Schepernisse and Maas (2009)	Figure 2
Capillary pressure p_c	Schepernisse and Maas (2009)	Equation 2
Aquifer thickness h	12 m	12 m
Anisotropy A	3	10
Extent r_m	Unknown	Quasi infinite (100 km radius)
Temperature gradient	3.7 °C/100m	3.5 °C/100m
Vertical pressure gradient	1.1 bar/10m	1.1 bar/10m
Depth	642 m	1000 m
Salinity	24 w/w%	20 w/w%
Injection regime	Variable	Pressure controlled
Max. injection overpressure p	22.9 bar	20 bar

Table 3: Model parameters for the central point and variation.

Parameters	Central point of sensitivity study	Scenarios
Discretisation (inner cells)	1 m	0.1 m, 0.5 m, 5 m
Model extent (radius), r_m	100 km	10 km, 1000 km
Well diameter, d	21.59 cm	5 cm, 10 cm
Permeability, K	100 mD	10 mD, 1000 mD
Hysteresis	Not applied	See Figure 2 and Equation 2
Aquifer thickness h	12 m	6 m, 24 m
Anisotropy. A	10	1, 1000
Depth	1000 m	650 m, 2000 m
Rock compressibility, S	7.2 10^{-5} bar^{-1}	None, 7.2 10^{-6} bar^{-1}, 7.2 10^{-4} bar^{-1}
Max. injection overpressure p	20 bar	1 bar, 40 bar
Injection regime	Pressure controlled	Power plant load curve controlled

Table 4: Sensitivities of model parameters. The central point parameters from Table 3 are applied. The injection rate as a function of the sensitivity is calculated by multiplication of the injection rate at the central point with the respective sensitivity term. The sensitivity term is the product of all sensitivities. The scale of the values is presented in the right two columns.

Input parameter	Min Max	Output rate [t/d]	Numerical Evaluation Linear Sensitivity	Numerical Evaluation Nonlinear Sensitivity	Analytical Evaluation Linear Sensitivity	Analytical Evaluation Nonlinear Sensitivity	Injection regime	Value range numeric/analytic	
Pressure p	0 40	$\overline{\dot{m}}(p)$	$\overline{\dot{m}}_{num,cp}\ 0.0536\ p$	$\overline{\dot{m}}_{num,cp}\ 0.0453\ p^{1.04}$	$\overline{\dot{m}}_{a,cp}\ 0.0542\ p$	$\overline{\dot{m}}_{a,cp}\ 0.0313\ p^{1.158}$	pressure controlled	0 2.14	0 2.25
	0 40		$\overline{\dot{m}}_{num,pp}\ 0.0523\ p$	$\overline{\dot{m}}_{num,pp}\ 0.0396\ p^{1.08}$	-	-	power plant controlled	0 2.12	
Time t	1 7300	$\dot{m}(t)$	-	$\overline{\dot{m}}_{num,cp}\ 0.8475\ t^{0.0209}$	-	$\overline{\dot{m}}_{a,cp}\ 1.071\ t^{-0.0089}$	pressure controlled	0.85 1.02	0.99 1.06
	365 7300		-	$\overline{\dot{m}}_{num,pp}\left(0.809-\frac{20.8}{t}+0.0251\ln(t)\right)$	-	-	power plant controlled	0.9 1.03	
Well Diameter d	5 21.59	$\overline{\dot{m}}(d)$	$\overline{\dot{m}}_{num,cp}\begin{pmatrix}0.955+\\2.13\ 10^{-3}\ d\end{pmatrix}$	$\overline{\dot{m}}_{num,cp}\ 0.925\ d^{0.0255}$	$\overline{\dot{m}}_{a,cp}\begin{pmatrix}0.001356+\\0.971\,d\end{pmatrix}$	$\overline{\dot{m}}_{a,cp}\ 0.951\ d^{0.016}$	pressure controlled	0.96 1	0.98 1
Depth D	650 2000	$\overline{\dot{m}}(D)$	$\overline{\dot{m}}_{num,cp}\begin{pmatrix}0.501+\\4.62\,10^{-4}\ D\end{pmatrix}$	$\overline{\dot{m}}_{num,cp}\ 0.0258\ D^{0.528}$	$\overline{\dot{m}}_{a,cp}\begin{pmatrix}6.98\cdot10^{-4}+\\0.1003\,D\end{pmatrix}$	$\overline{\dot{m}}_{a,cp}\,2.68(632-D)^{0.29}$	pressure controlled	0.79 1.43	0.42 1.46
Permeability K	10 1000	$\overline{\dot{m}}(K)$	$\overline{\dot{m}}_{num,cp}\ 0.0102\ K$	-	$\overline{\dot{m}}_{a,cp}\ 0.0097\ K$	$\overline{\dot{m}}_{a,cp}\ 0.0105\,K^{0.9885}$	pressure controlled	0.1 10.2	0.1 9.7
Aquifer thickness h	6 24	$\overline{\dot{m}}(h)$	$\overline{\dot{m}}_{num,cp}\ 0.0842\ h$	-	$\overline{\dot{m}}_{a,cp}\ 0.0833\,h$	-	pressure controlled	0.51 2.02	0.5 2
Anisotropy A	1 1000	$\overline{\dot{m}}(A)$	-	$\overline{\dot{m}}_{num,cp}\,1.03\ A^{-0.0118}$	-	-	pressure controlled	1.03 0.95	
Rock compressibility S	0 7.2 10^{-4}	$\overline{\dot{m}}(S)$	$\overline{\dot{m}}_{num,cp}\begin{pmatrix}0.913+\\549\ S\end{pmatrix}$	$\overline{\dot{m}}_{num,cp}\left(0.885+76.7\ S^{0.705}\right)$	$\overline{\dot{m}}_{a,cp}\begin{pmatrix}0.889+\\827.7\ S\end{pmatrix}$	$\overline{\dot{m}}_{a,cp}\left(0.821+44.77\ S^{0.579}\right)$	pressure controlled	0.89 1.35	0.87 1.5

13 Figures

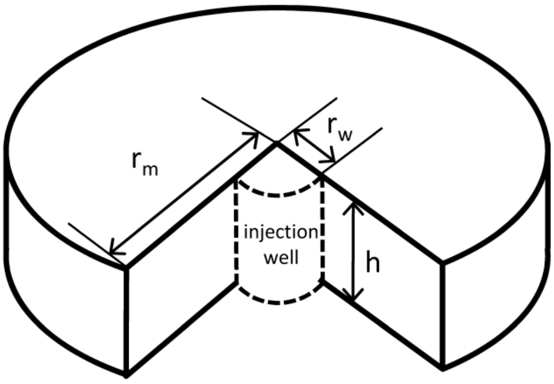

Fig. 1. Model domain of the numerical models. The model is 2-D radially symmetric, r_w is the radius of the injection well, r_m the radius of the model domain, h denotes the thickness of the aquifer. Except for the injection well all boundaries are no flow.

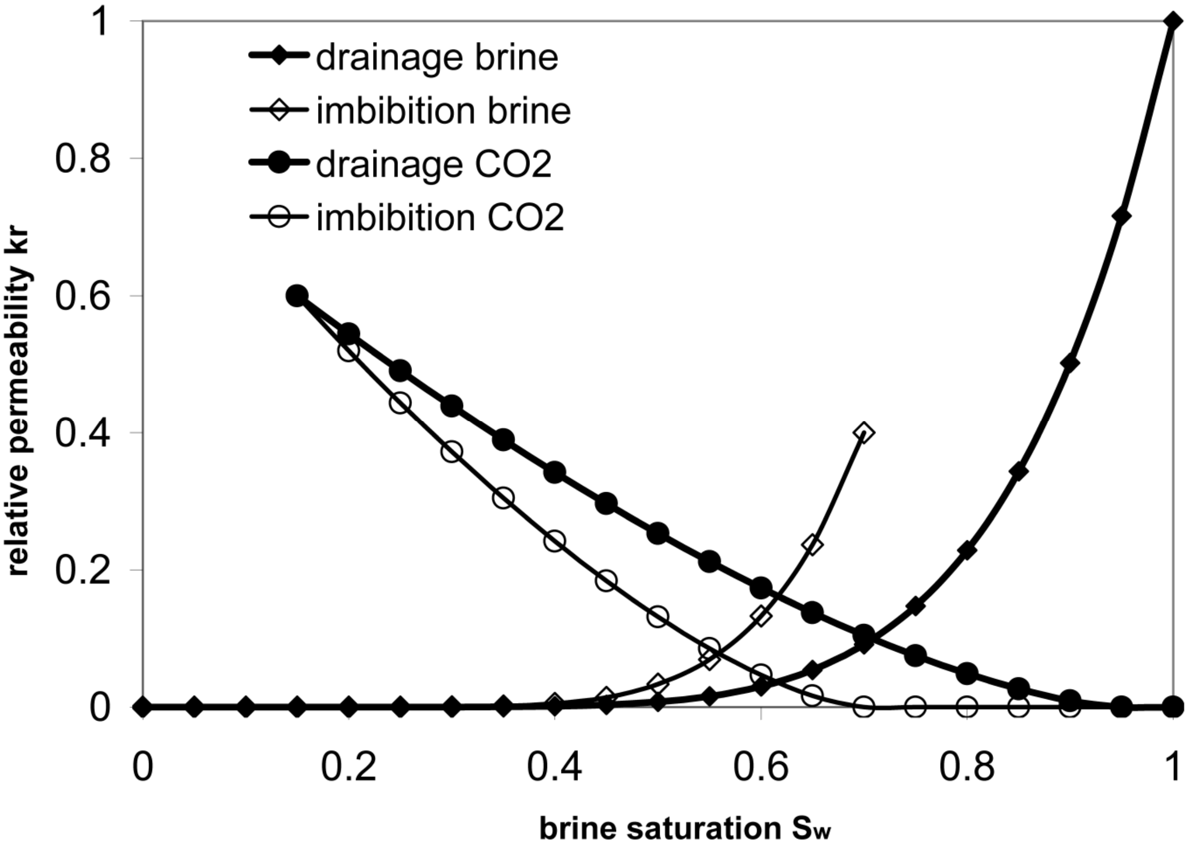

Fig. 2. Relative permeabilities of brine and CO_2. Residual brine saturation is 15%.

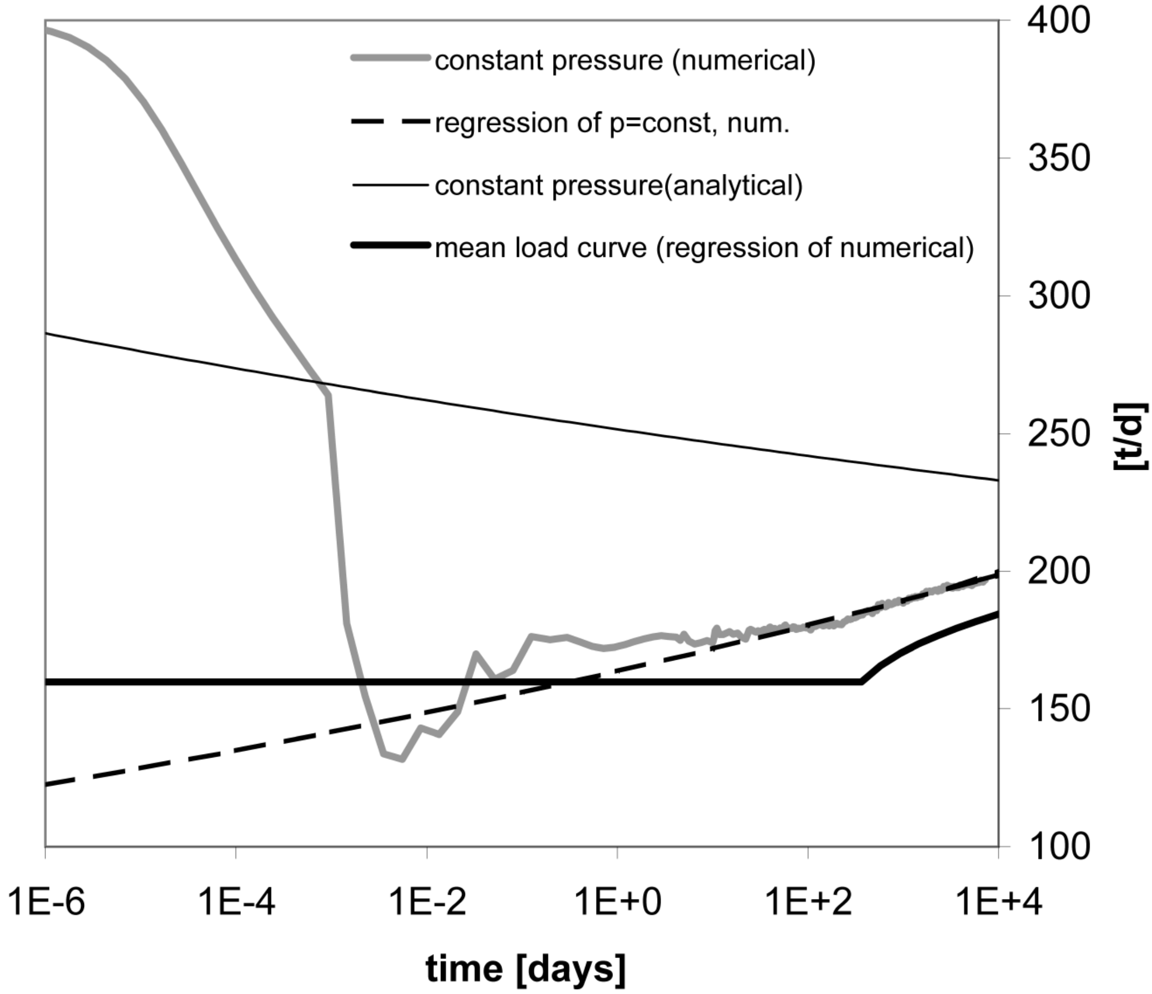

Fig. 3. Temporal injection rate at the central point, calculated with the numerical model and the analytical solution. The regression function corresponds to the numerical model.